




Article

A Mechanism Assessment and Differences of Cadmium Adsorption on Raw and Alkali-Modified Agricultural Waste

Marija Simić ^{1,*} , Jelena Petrović ¹ , Tatjana Šoštarić ¹, Marija Ercegović ¹, Jelena Milojković ¹, Zorica Lopičić ¹ 
and Marija Kojić ²

¹ Institute for Technology of Nuclear and Other Mineral Raw Materials, Franchet d'Espèrey 86, 11000 Belgrade, Serbia

² Institute of Nuclear Sciences "Vinča", University of Belgrade, 11000 Belgrade, Serbia

* Correspondence: m.petrovic@itnms.ac.rs; Tel.: +381-62-276-846

Abstract: In this study, raw corn silk was considered for the removal of cadmium ions from aqueous solutions. In order to improve adsorption characteristics, the KOH treatment was applied as a route to obtain modified materials. Both materials before and after metal adsorption were characterized by pH_{PZC}, SEM-EDX and FTIR analysis. SEM images and FTIR spectra revealed that alkali modification caused some structural changes that could improve the adsorption properties of the investigated material. The experimental results and the ion-exchange study revealed that the biosorption process of cadmium ions on to raw and modified corn silk was caused predominantly by the ion-exchange mechanism, followed by chemisorption. The kinetic parameters implied that there are three stages in the biosorption process. In addition, the cadmium adsorption on both materials is very fast and is followed by the pseudo-second-order kinetic model. The experimental results were fitted by two and three parameter isotherm models, while the Sips isotherm model best describes the biosorption process on both materials. According to the Sips isotherm model, the maximum adsorption capacity of cadmium adsorbed on modified materials was 49.06 mg g⁻¹, which is 2.23 times greater in comparison to the raw material (21.96 mg g⁻¹). Furthermore, the mechanisms of cadmium adsorption onto the investigated materials are summarized in order to better understand the modification influence on the adsorption properties of corn silk. In order to examine reusability of the investigated material, diluted nitric acid was used for regeneration. A desorption study was performed in three adsorption-desorption cycles. A high desorption efficiency (>85%) indicated that MCS after Cd adsorption can be efficiently recovered and reused for a new adsorption cycle.

Keywords: agricultural waste; alkali modification; adsorption process; heavy metals removal; mechanism assessment



Citation: Simić, M.; Petrović, J.; Šoštarić, T.; Ercegović, M.; Milojković, J.; Lopičić, Z.; Kojić, M. A Mechanism Assessment and Differences of Cadmium Adsorption on Raw and Alkali-Modified Agricultural Waste. *Processes* **2022**, *10*, 1957. <https://doi.org/10.3390/pr10101957>

Academic Editor: Javier Remon

Received: 7 September 2022

Accepted: 20 September 2022

Published: 28 September 2022

Publisher's Note: MDPI stays neutral with regard to jurisdictional claims in published maps and institutional affiliations.



Copyright: © 2022 by the authors. Licensee MDPI, Basel, Switzerland. This article is an open access article distributed under the terms and conditions of the Creative Commons Attribution (CC BY) license (<https://creativecommons.org/licenses/by/4.0/>).

1. Introduction

Released nonessential and toxic heavy metals such as mercury, lead and cadmium represent a serious threat for the environment and for living organisms. Heavy metals are not degradable, and their accumulation in the food chain may cause serious health problems or death. Cadmium is one of the heavy metals which is heavily used in many industries (electroplating, battery, plastic and paint pigments, etc.). Lymburner, 1974 noted that the use of cadmium products has expanded at a rate of 5–10% annually, and their potential spread is still very high [1]. An example is a province in southwest China, where there are a lot of mining and smelting industries. This has caused an increase in heavy metal pollution, especially cadmium pollution, over the past decade [2]. Due to its high toxicity and potential environmental problems, it is important to find an adequate solution for the removal of cadmium from industrial wastewaters.

Different conventional techniques (chemical precipitation, ion-exchange, membrane filtration, solvent extraction, etc.) are used for the removal of heavy metals from wastewaters.

However, all of the above-mentioned methods for wastewater treatment have disadvantages such as high operation costs, generation of toxic sludge and low selectivity and efficiency [3]. For that reason, the development of an alternative method for heavy metals removal has gained a lot of attention from the scientific community. Biosorption (usage of natural waste materials as pollutant adsorbents) has been found to be a promising technology for heavy metals removal from the wastewater. Availability, low cost, eco-friendly, and high efficiency are the main advantages of utilization of waste biomaterials as adsorbents [4–8].

Large-scale corn production generates huge amounts of waste materials that have been left behind in open landfill sites in the form of corn stalks, corn cobs, corn silk, tassels and leaves. Some of these wastes can be used in the biodiesel industry or as a source of energy. Corn silk, however, does not have an effective utilization. Due to its chemical structure, corn silk has good adsorption characteristics for heavy metals removal. Previous investigations revealed that corn silk is suitable for lead, copper and zinc adsorption from water solutions [9,10]. Nevertheless, the ability of corn silk for Cd^{2+} ions adsorption has not been previously considered. Alternatively, a simple and relatively low-cost modification method could probably improve the adsorption properties of corn silk. For that reason, an alkali treatment with 1M KOH was used for corn silk modification. The physicochemical characteristics of raw corn silk (CS) and alkali-modified corn silk (MCS) before and after Cd^{2+} adsorption were investigated by using different instrumental techniques that included: Fourier Transform Infrared Spectroscopy (FTIR), Scanning Electron Microscopy and energy-dispersive X-ray analysis (SEM-EDX). The effect of the solution pH, the initial metal concentration and the contact time were considered in order to understand the equilibrium, kinetics and mechanism of the adsorption process of Cd^{2+} on the investigated materials. The point of zero charge (pH_{PZC}) in the metal ion solution was determined in order to investigate the specific sorption of Cd^{2+} onto the adsorbents' surfaces.

The objectives of this study were: (i) to investigate the possibility of CS and MCS to remove Cd^{2+} from water solution, (ii) to study the Cd^{2+} adsorption kinetics on the CS and MCS using the pseudo- first and second-order models and the intra-particle diffusion model, (iii) to study the Cd^{2+} equilibrium adsorption on the CS and MCS using two and three parameter isotherm models: Langmuir, Freundlich, Sips, Redlich-Peterson, Dubinin-Radushkevich and Temkin, (iv) to determine the Cd^{2+} adsorption mechanisms onto CS and MCS. In addition, the differences between Cd^{2+} adsorption on the CS and MCS were also adopted in order to attribute innovative and novel explanations as to how much the metal adsorption process is influenced by the quantity of exchangeable cations, functional groups and physical properties of the material.

2. Materials and Methods

Corn silk was obtained from a corn field near Belgrade, Serbia. The pure material was washed with water and dried, and then milled, sieved and dried until constant weight. The prepared raw material (CS) was then used for adsorption experiments.

Alkali modification was carried out by stirring 2 g of the obtained CS with 200 mL of 1M KOH for 60 min at room temperature. The modified material was filtered through filter paper, washed with distilled water (pH neutral) and dried until constant weight. The prepared modified material (MCS) was used for adsorption experiments.

A stock Cd^{2+} solution (1000 mg L^{-1}) was prepared by dissolving $2.7443 \text{ g Cd}(\text{NO}_3)_2 \cdot 4\text{H}_2\text{O}$ (p.a. grade) in 1 L double distilled water (Sartorius, arium[®]pro, Goettingen, Germany). Working Cd^{2+} solutions of different concentrations (from 10 to 250 mg L^{-1}) were prepared by diluting the stock solution. The pH value of each solution was adjusted at 5.0 by adding small volumes of 0.01 M HNO_3 and/or 0.01 M KOH and monitored using a pH meter (SensIon MM340, HACH, Loveland, CO, Waltham, MA, USA).

The determination of the pH_{PZC} of CS and MCS in the KNO_3 solution (0.001 mol L^{-1}) was described in our previous study [9–11]. The pH_{PZC} of the CS and MCS in the metal ion solution was determined by the following: the initial pH values (pH_i) of Cd^{2+} solution

(0.001 mol L⁻¹) were adjusted to a range from 2.0 to 7.0 by adding 0.01 M HNO₃ and/or 0.01 M KOH. In 50 mL of each metal ion solution 0.05 g of adsorbent was added. Suspensions were stirred during 24 h (250 rpm), filtered through filter paper and the final pH value of solutions was measured (pH_f).

Surface morphology of the CS and MCS before and after Cd²⁺ adsorption was performed on a JEOL JSM-6610 LV SEM Scanning Electron Microscope (SEM) (JEOL Inc., Peabody, MA, USA), while the quantitative elemental composition of the CS and MCS surface, before and after adsorption, was analysed using energy-dispersive X-ray analysis (EDX) (JEOL Inc., USA). The samples were coated with gold before the analysis.

The functional groups of the CS and MCS before and after Cd²⁺ adsorption were analysed using a Thermo Nicolet 6700 FT-IR Spectrophotometer (Thermo Fisher Scientific, Waltham, MA, USA). The pastilles were prepared by mixing 0.8 mg of CS and MCS with 80 mg KBr.

Adsorption experiments of Cd²⁺ removal from water samples on the CS and MCS were performed in a batch system. In 100 mL Erlenmeyer flasks, an amount of 1 g L⁻¹ of adsorbent was added to metal solutions of different Cd²⁺ ion concentrations (from 10 to 250 mg L⁻¹). The suspensions were stirred in a mechanical shaker at 250 rpm during different contact times (from 2 to 180 min) and filtered through filter paper. The concentration of Cd²⁺ ions in the solutions was determined by an Atomic Adsorption Spectrophotometer (PerkinElmer, PinAAcle 900T, Waltham, MA, USA).

The amount of adsorbed Cd²⁺ on the adsorbent in equilibrium and at the time t , was calculated by Equations (1) and (2), respectively:

$$q_e = (C_0 - C_e) \cdot V / m \quad (1)$$

$$q_t = (C_0 - C_t) \cdot V / m \quad (2)$$

where: q_e and q_t are the amount of adsorbed Cd²⁺ ion in equilibrium and at the time t , respectively (mg g⁻¹); C_0 is the initial Cd²⁺ ion concentration (mg L⁻¹); C_e and C_t are the Cd²⁺ ion concentration in equilibrium and at the time t , respectively (mg L⁻¹); V is the volume of Cd²⁺ ion solution (L); and m is the mass of the adsorbent (g).

In order to examine the ion-exchange mechanism, the materials were shaken for 2 h at 250 rpm. Experiments were performed at three different Cd²⁺ concentrations (20, 60 and 100 mg L⁻¹). Then, suspensions were filtered through filter paper and a concentration of Cd²⁺, K⁺, Na⁺, Mg²⁺ and Ca²⁺ was measured by AAS, while H⁺ concentration was calculated based on the difference in the pH value between the control and final samples.

A desorption study was performed in a batch system. MCS was shaken in a cadmium ion solution for 2 h at room temperature, filtered and rinsed with double distilled water to remove non-adsorbed cadmium ions. After that, cadmium-loaded MCS was mixed with 0.1 mol L⁻¹ HNO₃ and shaken for 2 h, then filtered and rinsed several times with double distilled water. The adsorption/desorption experiments were performed in three cycles. The concentration of cadmium ions in solutions was measured by an Atomic Adsorption Spectrophotometer (PerkinElmer, PinAAcle 900T).

All experiments were done in triplicate.

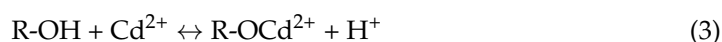
3. Results and Discussion

3.1. Adsorbent Characterization

3.1.1. Specific Sorption

Specific sorption of Cd²⁺ on the CS and MCS was confirmed by comparing the value of pH_{PZC} in both KNO₃ and Cd (NO₃)₂ solutions. In the KNO₃ solutions, it was found that the value of pH_{PZC} is higher after alkali modification (CS and MCS were 6.0 [10] and 7.7, respectively), indicating that during the KOH treatment, the SC surface become more alkaline. This was probably due to the increase of content of -OH functional groups. However, after equilibrium with the Cd²⁺ solution, the pH_{PZC} decreased to 5.2 and 6.6 for CS and MCS, respectively. This indicates that during the sorption of Cd²⁺ ions onto

functional groups of CS and MCS, hydrogen ions are released into solutions, lowering the pH_{PZC} of both sorbents (Figure 1). Comparing these values with those obtained for the same solid/liquid ratio in the KNO_3 solution, it can be concluded that the decrease in pH_{PZC} after Cd^{2+} adsorption involved specific sorption as the binding mechanism [12]. Keeping in mind that the adsorption experiments were done at $pH < 6.0$, where the surfaces of CS and MCS are positively charged, the electrostatic forces are not responsible for Cd^{2+} adsorption onto the investigated materials, but by the specific sorption through the complex in the forms (sorbent-O)- Cd^+ or (sorbent-O) $_2$ -Cd. The fact that the sorption of Cd^{2+} ions on both CS and MCS occurs in solutions with pH values much below the value of pH_{PZC} , indicates the formation of bonds between the adsorbed species and the sorbents' surface oxygen groups, or the precipitation of hydroxides on the sorbents' surfaces [12]. The binding mechanism could be explained by the following equation:



where: R-OH is the functional group of the CS and MCS.

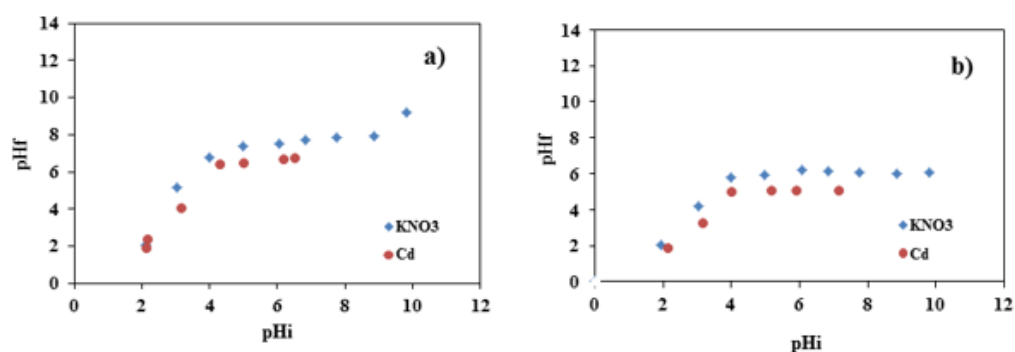


Figure 1. pH_{PZC} in KNO_3 and Cd^{2+} solution for CS (a) and MCS (b).

3.1.2. SEM-EDX Analysis

The SEM micrograph (1000 times magnification) and the EDX spectrum of the CS and MCS before and after Cd^{2+} adsorption are shown in Figure 2.

As can be seen (Figure 2a), the pristine CS had continuous and flat surfaces with notable micron-size channels that was explained in our previous studies [9,10]. On the contrary, alkali modification could increase surface porosity of different materials and clean up partially blocked pores [13]. It is also known that the alkali treatment caused degradation of the structural constituents of lignocellulosic materials (cellulose, hemicellulose etc.) [14,15]. Accordingly, the smooth structure of CS after the alkaline treatment becomes significantly disarranged (Figure 2b). The obtained modified material exhibits a much rougher, heterogeneous surface with clearly notable cracks and pores which provides more electron-donating sites for Cd^{2+} binding. This is in accordance with experimentally obtained results in this study that showed a higher adsorption capacity of MCS in comparison to untreated CS. A similar observation was previously reported by Šoštarić et al., 2018 [15], who found that apricot shells exhibit a better adsorption capacity for Cu^{2+} , Pb^{2+} and Zn^{2+} removal after NaOH treatment [15].

In addition to previous findings, Figure 2c,d showed the absence of microprecipitation during biosorption of Cd^{2+} , since there are no visible aggregates of cadmium ions on the CS and MCS surface. The EDX spectrum of the MCS exhibited the more pronounced K peak in comparison to the CS, suggesting that K was integrated on the material surface during the KOH treatment. Furthermore, after Cd^{2+} biosorption, this peak almost completely disappeared while the peaks of Cd were observed (Figure 2d). This implied involvement of K ions into the metal binding mechanism and thus enhanced the adsorption performance of the material after KOH modification. Summarising our findings, it can be concluded that KOH modification improves the adsorption abilities of CS due to increasing the surface

area, providing more K ions which are involved in the ion-exchange mechanism with Cd^{2+} ions as well as more electro-donating sites for Cd^{2+} binding.

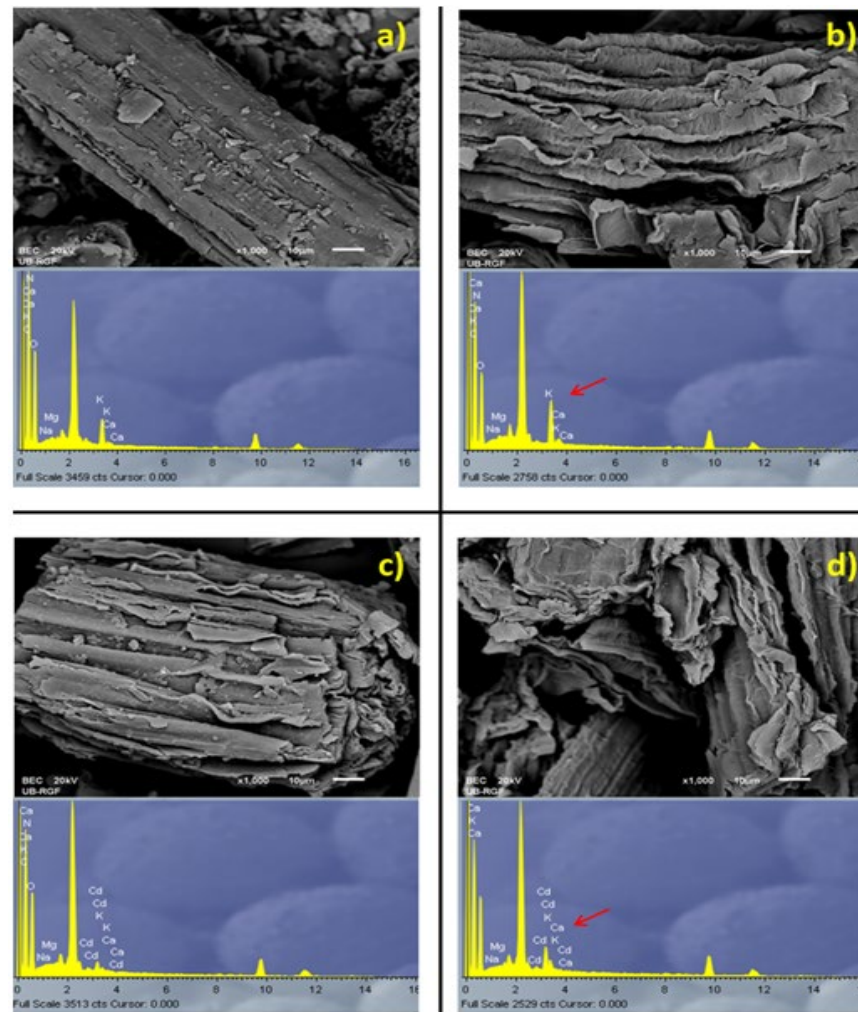


Figure 2. SEM micrograph and EDX spectrum of the CS (a) and MCS (b) before and the CS (c) and MCS (d) after Cd^{2+} adsorption.

3.1.3. FT-IR Analysis

The FT-IR spectra of the CS, MCS and MCS after Cd adsorption are shown in Figure 3.

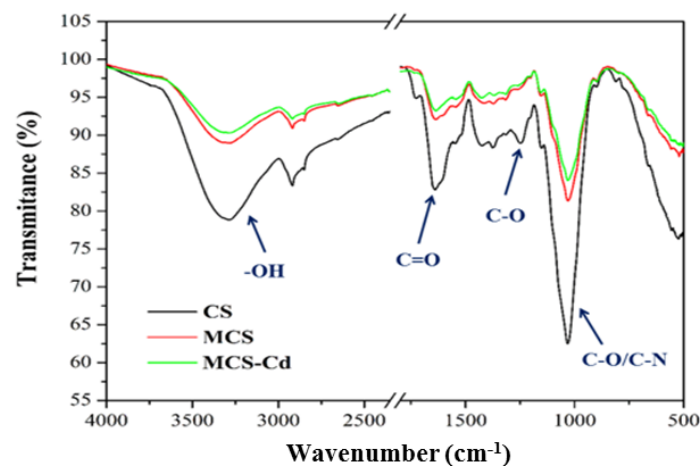


Figure 3. FTIR spectra of the CS and MCS before and after Cd^{2+} adsorption.

The characteristic peaks of the CS were reported in detail in our previous study [10]. As can be seen from Figure 3, alkali modification caused some changes in the CS structure. It is notable that the intensity of all peaks in FTIR spectra becomes less pronounced after KOH treatment. The major structural changes upon modification were confirmed by the disappearance of C-O band at 1250 cm^{-1} , and the visible decrease in intensity of -OH, C=O and C-N/C-O bands at 3287 , 1637 and 1032 cm^{-1} , respectively (Figure 3). Observed changes in FTIR spectra caused by alkali treatment are probably a result of degradation of the lignocellulosic constituents of the CS. A similar trend was previously observed during modification of apricot shells with NaOH [15].

Conversely, as a result of Cd^{2+} adsorption on the MCS, some of the peaks in the FTIR spectra showed a decreased intensity (-OH, C=C, C-N), while peaks attributed to -OH, C-O, C-O-C and C=C bands were shifted to the lower wavenumbers (Figure 3). This suggests their involvement in Cd^{2+} adsorption on the MCS by ion-exchange and chemisorption [9,16].

3.2. Kinetic Study

In order to describe the adsorption kinetics of Cd^{2+} on the CS and MCS, the experimental results were fitted by the three kinetic models chosen: pseudo-I-order, pseudo-II-order and the intraparticle diffusion model. The pseudo-I-order model, pseudo-II-order model and the intraparticle diffusion model can be expressed as Equations (4)–(6), respectively [17–19]:

$$1/q_t = 1/q_e + k_1/q_e t \quad (4)$$

$$t/q_t = 1/k_2 q_e^2 + t/q_e \quad (5)$$

$$q_t = k_{id} t^{1/2} + C \quad (6)$$

where: k_1 and k_2 are the pseudo-I-order and pseudo-II-order rate constant (min^{-1}), respectively; k_{id} is the intraparticle diffusion rate constant ($\text{mg g}^{-1} \text{min}^{-1/2}$), and C is intercept.

Based on the slopes and intercepts from linear plots (Figure 4), the kinetic parameters and coefficients of determination (R^2) were obtained.

Table 1 presents the parameters obtained from kinetic models, as well as the values of R^2 for adsorption of Cd^{2+} on the CS and MCS.

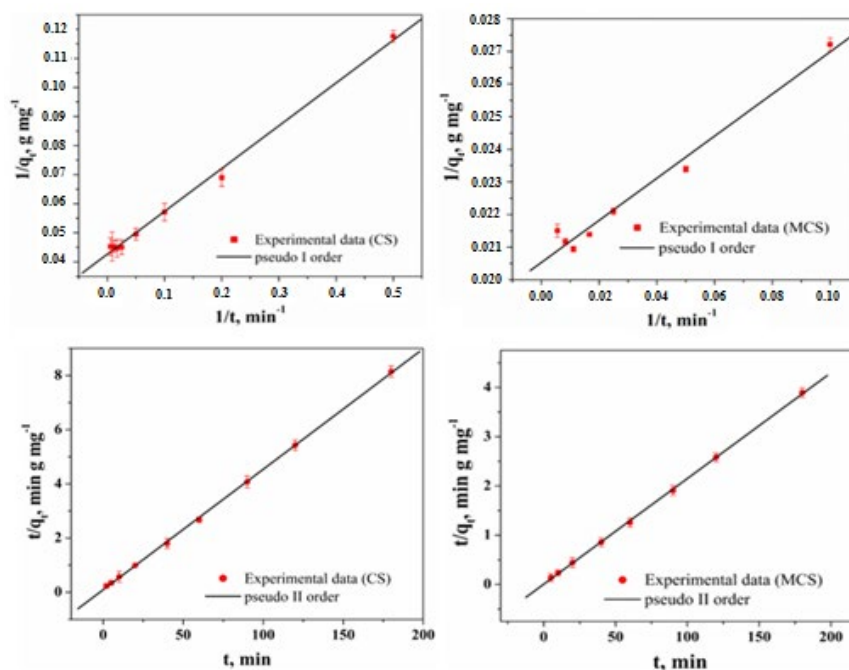


Figure 4. Cont.

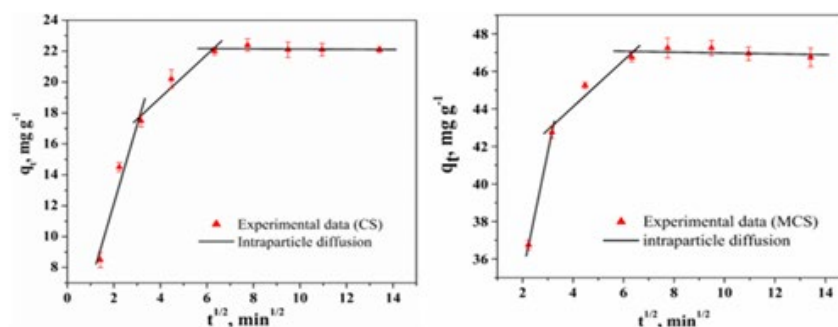


Figure 4. Kinetic models for Cd^{2+} adsorption on the CS and MCS.

Table 1. Kinetic parameters for Cd^{2+} adsorption on the CS and MCS.

| Kinetics Model | CS | MCS |
|---|-------------------|-------------------|
| $q_{e,exp}$ | 22.4 ± 0.52 | 46.79 ± 0.98 |
| Pseudo-I-order | | |
| $q_{e,cal}$ | 23.46 ± 0.75 | 48.71 ± 0.98 |
| k_1 (min^{-1}) | 3.456 ± 0.06 | 3.14 ± 0.12 |
| R^2 | 0.996 | 0.996 |
| Pseudo-II-order | | |
| $q_{e,cal}$ (mg g^{-1}) | 22.5 ± 0.63 | 46.62 ± 1.05 |
| k_2 ($\text{g mg}^{-1} \text{min}^{-1}$) | 0.021 ± 0.001 | 0.095 ± 0.002 |
| R^2 | 0.999 | 0.999 |
| Intra particle diffusion | | |
| k_{i1} ($\text{mg g}^{-1} \text{min}^{-1/2}$) | 5.11 ± 0.03 | 6.48 ± 0.02 |
| R_{i1}^2 | 0.97 | 1 |
| k_{i2} ($\text{mg g}^{-1} \text{min}^{-1/2}$) | 1.39 ± 0.01 | 1.23 ± 0.05 |
| R_{i2}^2 | 0.98 | 0.97 |
| k_{i3} ($\text{mg g}^{-1} \text{min}^{-1/2}$) | 0.007 ± 0.001 | 0.023 ± 0.001 |
| R_{i3}^2 | 0.134 | 0.25 |

As can be seen from Table 1, the value of $q_{e,cal}$ from the pseudo-II-order model is very close to the value of $q_{e,exp}$, and also the value of R^2 is very high (0.999). It indicates that the pseudo-II-order kinetic model well describes biosorption process of Cd^{2+} on the CS and MCS. These results suggest that the chemisorption process is involved in the biosorption of Cd^{2+} on both of the tested materials [20–22]. This assumption was in accordance with previously results from this study (FTIR/pHpzc). Additionally, the curve (q_t vs. $t^{1/2}$) showed multilinearity (Figure 4), indicating that more than one step is involved in the adsorption process of Cd^{2+} onto the investigated materials. These steps include: (i) diffusion of Cd ions through a solution to the surface of CS and MCS (first region); (ii) intraparticle diffusion of Cd ions (second step); and (iii) the equilibrium stage (third step). A similar observation was previously described by Cheung et al. [23].

3.3. Adsorption Isotherm Study

The experimental results were fitted by different isotherm models in order to describe the equilibrium of biosorption process of Cd^{2+} ions on the CS and MCS. Two parameter isotherm models (Langmuir, Freundlich, Dubinin–Radushkevich and Tempkin) and three parameter isotherm models (Sips and Redlich–Peterson) were used.

The Langmuir isotherm model is valid for monolayer adsorption where the sorption of species can occur only at a fixed number of energetically equivalent sites. This model was used in order to get information about the maximum biosorption capacity of the biosorbent. The Langmuir isotherm model can be expressed as the following equation [24]:

$$q_e = q_{max} K_L C_e / (1 + K_L C_e) \quad (7)$$

where: q_{max} is the maximal amount of adsorbed Cd^{2+} on the CS and MCS ($mg\ g^{-1}$), and K_L is the Langmuir constant ($L\ mg^{-1}$).

The dimensionless constant (R_L) which describes the feasibility of the Langmuir isotherm model and favorability of the biosorption process can be expressed by the following equation [25]:

$$R_L = 1/(1 + K_L C_0) \quad (8)$$

where: R_L is separation factor. The biosorption process of Cd^{2+} on the CS and MCS is: unfavorable if the $R_L > 1$; linear if the $R_L = 1$; favorable if the $0 < R_L < 1$ or irreversible if the $R_L = 0$ [26].

The Freundlich isotherm model is valid for multilayer adsorption where the sorption process occurs at the heterogeneous surface. This model can be expressed as the following equation [27]:

$$q_e = K_F C_e^{1/n_F} \quad (9)$$

where: K_F is the Freundlich constant ($mg\ g^{-1}\ (mg\ L^{-1})^{-1/n}$) and $1/n_F$ is an empirical Freundlich parameter. The biosorption process of Cd^{2+} on the CS and MCS is favorable if the value of n_F is between 1 and 10.

The Dubinin–Radushkevich isotherm model was used for the calculation of sorption energy. It can be expressed as the following equations [28]:

$$q_e = q_s \exp(-k_{DR} \varepsilon^2) \quad (10)$$

$$\varepsilon = RT \ln[1 + 1/C_e] \quad (11)$$

where: q_s is the theoretical isotherm saturation capacity ($mg\ g^{-1}$); k_{DR} is the Dubinin–Radushkevich constant ($mol^2\ kJ^{-2}$); ε is the Polanyi potential ($kJ^2\ mol^{-2}$); R is the gas constant ($8.314\ J\ (mol\ K)^{-1}$); and T is the absolute temperature (K).

The Temkin isotherm model gives information about the interaction between the investigated materials and Cd^{2+} ions, and can be expressed as the following equation [29]:

$$q_e = (RT/b_T) \ln K_T C_e \quad (12)$$

where: b_T is the Temkin constant related to the heat of biosorption and K_T is the equilibrium binding constant ($dm^3\ mol^{-1}$).

The Sips isotherm model is the combination of the Langmuir and Freundlich isotherm models: it approaches the Freundlich isotherm at low sorbate concentrations, while at high concentrations it predicts a monolayer adsorption capacity characteristic for the Langmuir isotherm. It can be expressed as the following equation [30]:

$$q_e = q_{max} (K_S C_e)^{1/n_S} / \left(1 + (K_S C_e)^{1/n_S} \right) \quad (13)$$

where: K_S is the Sips constant related to sorption affinity ($(mg\ L^{-1})^{-1/n}$) and $1/n_S$ is an empirical Sips parameter which indicates sorbent heterogeneity; a higher value of this parameter indicates a more heterogenous system.

The Redlich–Peterson isotherm model can be expressed as the following equation [31]:

$$q_e = K_{RP} C_e / (1 + a_{RP} C_e^g) \quad (14)$$

where: K_{RP} and a_{RP} are Redlich–Peterson constants ($L\ g^{-1}$) and $((mg\ L^{-1})^{-g})$, respectively, and g is an empirical Redlich–Peterson parameter ($g \leq 1$).

Equilibrium data were fitted to mentioned isotherm models, and the coefficient of determination (R^2) and nonlinear chi-square (χ^2) values were the criteria used for model selection. The isotherm models of Cd^{2+} adsorption on the CS and MCS are presented in Figure 5.

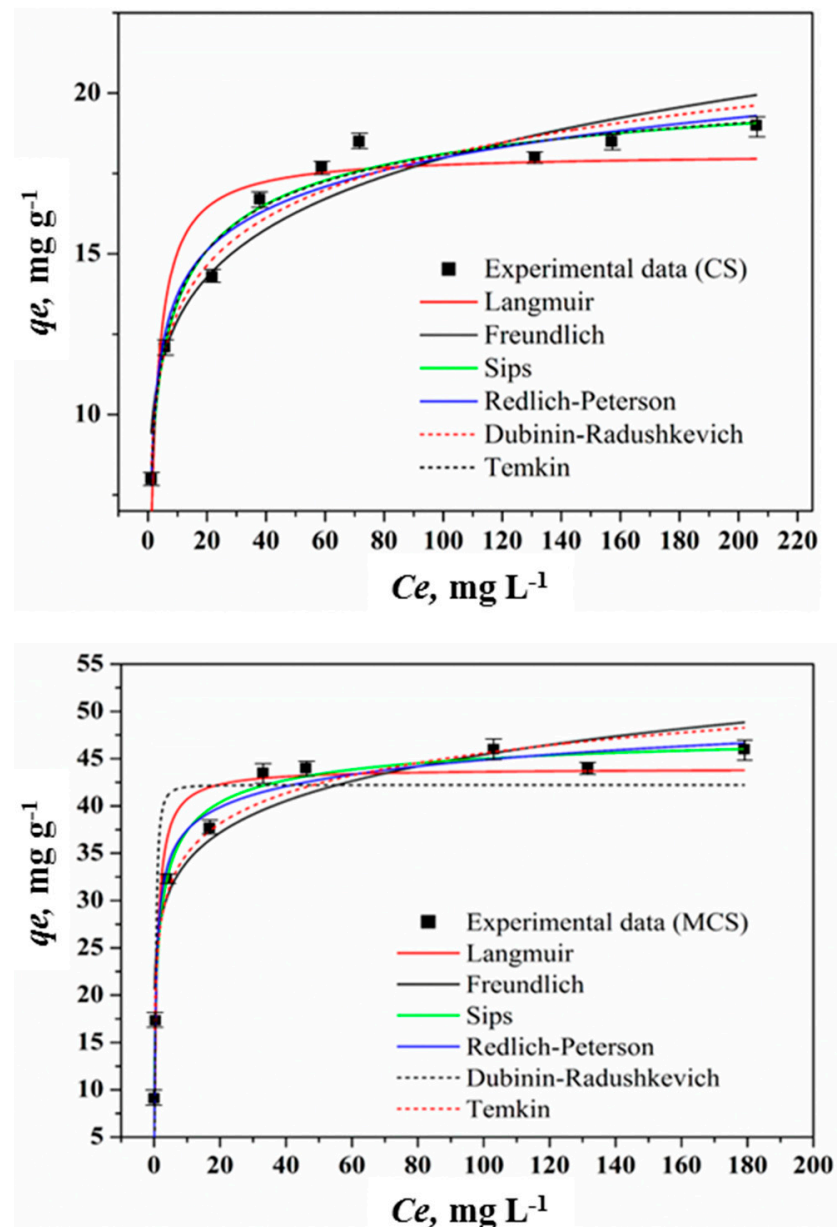


Figure 5. Isotherm models of Cd^{2+} adsorption on to CS and MCS.

Table 2 contains parameters of equilibrium models for Cd^{2+} biosorption on the CS, as well as the appropriate coefficient of determination (R^2) and nonlinear chi-square (χ^2) values.

The data presented in Table 2 demonstrates that the Langmuir equation provides a reasonable description of the experimental data, with 23.75 mg g^{-1} as the monolayer capacity of CS calculated at 25°C . Values of R_L (Langmuir constant) and n_F (Freundlich model) are between 0–1 and 0–10, respectively, indicating favourable biosorption of Cd^{2+} on the CS.

Based on the values of the R^2 and χ^2 it can be concluded that the Sips isotherm model best describes the biosorption of Cd^{2+} on the CS and MCS. According to this isotherm model, the maximum adsorption capacities for Cd^{2+} removal are 21.95 and 49.06 mg g^{-1} for CS and MCS, respectively. Besides, it can be seen that the Sips parameter $1/n_S$ is bigger than 1 for both investigated materials, indicating heterogeneity of the materials' surfaces.

Table 2. Isotherm parameters for Cd²⁺ biosorption on the CS.

| Isotherm Model | CS | MCS |
|--|----------------|---------------|
| Langmuir | | |
| q_{max} (mg g ⁻¹) | 18.13 ± 0.08 | 43.97 ± 1.07 |
| K_L (L mg ⁻¹) | 3.456 ± 0.02 | 3.14 ± 0.06 |
| R^2 | 0.996 | 0.996 |
| χ^2 | 1.689 | 9.07 |
| Freundlich | | |
| K_F (mg g ⁻¹ (mg L ⁻¹) ^{-1/nf}) | 9.29 ± 0.55 | 25.61 ± 0.87 |
| n_F | 6.97 ± 0.03 | 8.03 ± 0.06 |
| R^2 | 0.917 | 0.871 |
| χ^2 | 1.138 | 12.62 |
| Dubinin–Radushkevich | | |
| ϵ^2 | 1.79 | 6.4 |
| R^2 | 0.655 | 0.834 |
| χ^2 | 4.782 | 30.45 |
| Tempkin | | |
| K_T | 47.81 ± 1.21 | 194.13 ± 2.23 |
| b_T (KJ mol ⁻¹) | 1141.85 ± 5.13 | 527.7 ± 1.55 |
| R^2 | 0.959 | 0.907 |
| χ^2 | 0.566 | 17.11 |
| Sips | | |
| q_{max} (mg g ⁻¹) | 21.95 ± 0.53 | 49.06 ± 1.06 |
| K_S (mg L ⁻¹) ^{-1/ns} | 0.534 ± 0.004 | 0.921 ± 0.007 |
| n_S | 2.12 ± 0.04 | 1.85 ± 0.23 |
| R^2 | 0.97 | 0.956 |
| χ^2 | 0.402 | 5.44 |
| Redlich–Peterson | | |
| K_{RP} (L g ⁻¹) | 20.04 ± 0.92 | 96.38 ± 1.33 |
| a_{RP} (mg L ⁻¹) ^g | 1.67 ± 0.23 | 2.86 ± 0.41 |
| g | 0.909 ± 0.002 | 0.937 ± 0.005 |
| R^2 | 0.961 | 0.912 |
| χ^2 | 0.547 | 16.15 |

3.4. Mechanism Study

The ion-exchange mechanism is one of the dominant mechanisms involved in the adsorption process of metal ions [16,32]. In this study, the ion-exchange mechanism was investigated through the relation between the adsorbed Cd²⁺ and released cations (K⁺, Na⁺, Ca²⁺, Mg²⁺ and H⁺) from the CS and MCS during the biosorption process. The amount of adsorbed Cd²⁺ and released K⁺, Na⁺, Ca²⁺, Mg²⁺ and H⁺ are shown in Figure 6.

The relation between the amounts of adsorbed Cd²⁺ and released cations was calculated by the following equation [32,33]:

$$R_{b/r} = C_{Cd^{2+}} / [(C_{K^+} / 2) + (C_{Na^+} / 2) + C_{Mg^{2+}} + C_{Ca^{2+}} + (C_{H^+} / 2)] \quad (15)$$

Results are shown in Figure 6.

The replacement of K⁺, Na⁺, Ca²⁺ and Mg²⁺ indicates the formation of ionic binding, while replacement of H⁺ indicates the formation of covalent binding between Cd²⁺ and active sites on the CS and MCS during the adsorption process [33]. As can be seen (Figure 6), alkali modification improves the exchangeability of H⁺ ions as well as decreases the involvement of the ion-exchange mechanism in Cd²⁺ binding. It can be concluded that the KOH treatment promotes a covalent interaction between the metal ions and the material surface.

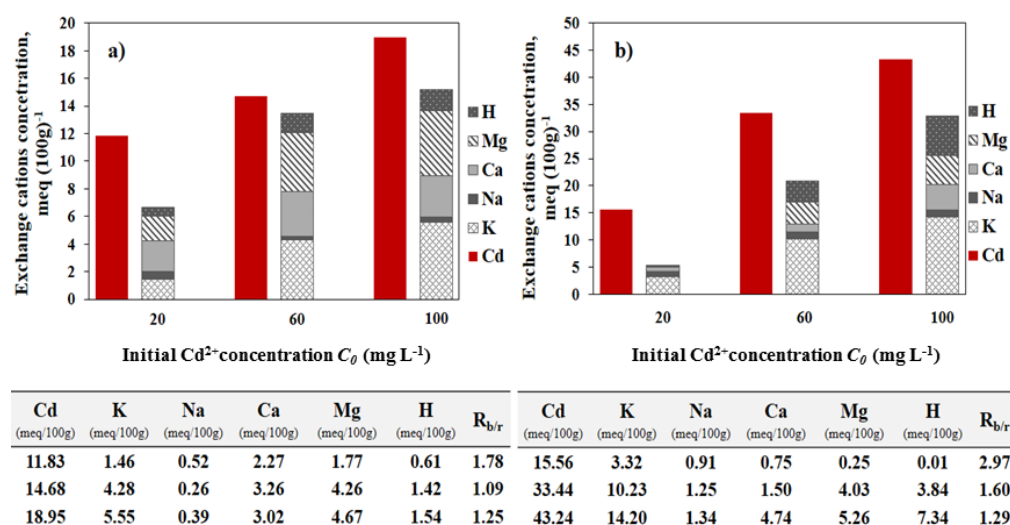


Figure 6. The amount of adsorbed Cd^{2+} and released K^+ , Na^+ , Ca^{2+} , Mg^{2+} and H^+ from CS (a) and MCS (b) during adsorption process.

The value of $R_{b/r}$ is >1 for all investigated Cd^{2+} concentrations, which means that the amount of released cations is smaller than the amount of adsorbed Cd^{2+} . This suggests that the ion-exchange mechanism is not the only one, but is the dominant mechanism during the adsorption of Cd^{2+} on the CS and MCS. Similar results were proposed by Gorgievski et al., 2013 [32]. As can be seen (Figure 6), the adsorbed Cd^{2+} is mainly exchanged with K^+ , Mg^{2+} and H^+ ions. Since K^+ ion is the most exchangeable cation during Cd adsorption on the CS, its integration during modification significantly improves the adsorption capacity of MCS. Afterwards, the exchangeability of Ca^{2+} , Mg^{2+} and H^+ ions at higher Cd concentrations become more pronounced after modification (Figure 6). These results indicate that KOH modification not only increases the K^+ ions content, but also improves exchangeability of other cations, making the material more available to Cd^{2+} ions. The involvement of the ion-exchange mechanism in Cd^{2+} biosorption on both of the investigated materials was previously confirmed in this study by EDX analysis (Figure 2).

Additionally, in summarizing the results from this study, it can be concluded that Cd^{2+} adsorption onto the investigated materials is a complex process which consists of different mechanisms that include: (i) the ion-exchange mechanism; (ii) the surface complexation between oxygen-functional groups on to the materials' surface and metal ions; and (iii) Cd^{2+} - π with electrons from $\text{C}=\text{C}$. Furthermore, a higher affinity of the material for cadmium ion is noticeable after alkaline modification; the surface becomes more accessible for the binding of the selected ion while the interaction ability and ion exchangeability are upgraded.

3.5. Desorption Study

In order to examine the reusability of MCS and recovery of the cadmium ions, a desorption study was performed in three adsorption/desorption cycles. Diluted HNO_3 was used as a desorption agent. The desorption efficiency after three cycles was more than 85%, indicating that MCS after cadmium adsorption can be efficiently regenerated and reused for a new adsorption cycle. Conversely, the adsorption capacity after three adsorption/desorption cycles decreased from 49.06 to 32.7 mg g^{-1} indicating that the Cd^{2+} adsorption on the MCS is a partially recoverable process.

4. Conclusions

The CS and MCS before and after Cd^{2+} adsorption were characterized by pH_{PZC} , SEM-EDX and FTIR analysis. The value of pH_{PZC} of CS and MCS was 6.0 and 7.7, respectively in a KNO_3 background solution, while it was 5.2 and 6.6, respectively in a Cd^{2+} ion solution. The decrease of pH_{PZC} in a metal ion solution indicated that cadmium ions were adsorbed

on CS and MCS by specific sorption. SEM images confirmed that MCS exhibits a much rougher, heterogeneous surface with clearly notable cracks and pores, compared to CS. FTIR spectra revealed that alkali modification caused some structural changes that could improve the adsorption properties of the investigated material.

The results of this study (ion-exchange study, SEM-EDX and FTIR analysis before and after Cd^{2+} adsorption and kinetic study) revealed that the biosorption process of Cd^{2+} on to CS and MCS was caused predominantly by the ion-exchange mechanism followed by chemisorption. The experimental results were fitted by Langmuir, Freundlich, Dubinin–Radushkevich, Tempkin, Sips and Redlich–Peterson isotherm models to describe the equilibrium of biosorption process of Cd^{2+} ions on to CS and MCS. The Sips isotherm model best describes the adsorption of Cd^{2+} on both materials. The calculated Cd^{2+} adsorption capacity of MCS (49.06 mg g^{-1}) was 2.23 time higher in comparison to the Cd^{2+} maximum adsorption capacity of CS (21.96 mg g^{-1}). In order to consider reusability of the investigated material, a desorption study using diluted nitric acid was performed. The obtained desorption efficiency of $>85\%$ implies that MCS after Cd^{2+} adsorption can be efficiently reused in several adsorption/desorption cycles.

In summary, the results of this study lead to the conclusion that the CS adsorption capacity for Cd^{2+} increases after its KOH modification due to:

- increased surface porosity of CS, and degradation of structural lignocellulosic constituents which provide more electron-donating sites for Cd^{2+} binding;
- more K ions onto CS surface which are involved in ion-exchange mechanism with Cd^{2+} ions as well as more electro-donating sites for Cd^{2+} binding;
- improved exchangeability of Ca^{2+} , Mg^{2+} and H^+ ions, which makes the material more available to Cd^{2+} ions binding and promotes covalent interaction between metal ions and the material surface.

Author Contributions: Conceptualization, M.S. and J.P.; methodology, M.S. and J.M.; software, M.K.; validation, T.Š., Z.L. and M.S.; formal analysis, M.E.; investigation, M.S.; resources, M.S. and J.M.; data curation, M.E.; writing—original draft preparation, M.S.; writing—review and editing, J.P. and M.E.; visualization, T.Š.; supervision, M.S.; project administration, Z.L.; funding acquisition, J.M. All authors have read and agreed to the published version of the manuscript.

Funding: This research was funded by the Serbian Ministry of Education, Science and Technological De-velopment (contract no. 451-03-68/2022-14/200023).

Institutional Review Board Statement: Not applicable.

Informed Consent Statement: Not applicable.

Data Availability Statement: Not applicable.

Acknowledgments: Not applicable.

Conflicts of Interest: The authors declare no conflict of interest.

References

1. Lymburner, D.B. The production, use and distribution of cadmium in Canada. In *Environ-Mental Contaminants Inventory Study No. 2*; Report Series no. 39; Centre for Inland waters (Directorate): Ottawa, ON, Canada, 1974.
2. Ma, X.; Yan, X.; Yao, J.; Zeng, S.; Wei, Q. Feasibility and comparative analysis of cadmium biosorption by living *Scenedesmus obliquus* FACHB-12 biofilms. *Chemosphere* **2021**, *275*, 130125. [[CrossRef](#)] [[PubMed](#)]
3. Solisio, C.; Al Arni, S.; Converti, A. Adsorption of inorganic mercury from aqueous solutions onto dry biomass of *Chlorella vulgaris*: Kinetic and isotherm study. *Environ. Technol.* **2019**, *40*, 664–672. [[CrossRef](#)] [[PubMed](#)]
4. Pap, S.; Radonić, J.; Trifunović, S.; Adamović, D.; Mihajlović, I.; Miloradov, M.V.; Turk Sekulić, M. Evaluation of the adsorption potential of eco-friendly activated carbon prepared from cherry kernels for the removal of Pb^{2+} , Cd^{2+} and Ni^{2+} from aqueous wastes. *J. Environ. Manag.* **2016**, *184*, 297–306. [[CrossRef](#)] [[PubMed](#)]
5. Hu, Y.; Guo, X.; Wang, J. Biosorption of Sr^{2+} and Cs^+ onto *Undaria pinnatifida*: Isothermal titration calorimetry and molecular dynamics simulation. *J. Mol. Liq.* **2020**, *319*, 114146. [[CrossRef](#)]
6. Basu, A.; Ali, S.S.; Hossain, S.K.S.; Asif, M. A Review of the Dynamic Mathematical Modeling of Heavy Metal Removal with the Biosorption Process. *Processes* **2022**, *10*, 1154. [[CrossRef](#)]

7. Morales-Barrera, L.; Cristiani-Urbina, E. Equilibrium Biosorption of Zn^{2+} and Ni^{2+} Ions from Monometallic and Bimetallic Solutions by Crab Shell Biomass. *Processes* **2022**, *10*, 886. [[CrossRef](#)]
8. Piekarski, J.; Ignatowicz, K.; Dąbrowski, T. Application of an Adsorption Process on Selected Materials, Including Waste, as a Barrier to the Pesticide Penetration into the Environment. *Materials* **2022**, *15*, 4680. [[CrossRef](#)]
9. Petrović, M.; Šoštarčić, T.; Stojanović, M.; Milojković, J.; Mihajlović, M.; Stanojević, M.; Stanković, S. Removal of Pb^{2+} ions by raw Corn silk (*Zea mays* L) as a novel biosorbent. *J. Taiwan Inst. Chem. E* **2016**, *58*, 407–416. [[CrossRef](#)]
10. Petrović, M.; Šoštarčić, T.; Stojanović, M.; Petrović, J.; Mihajlović, M.; Ćosović, A.; Stanković, S. Mechanism of adsorption of Cu^{2+} and Zn^{2+} on the corn silk (*Zea mays* L.). *Ecol. Eng.* **2017**, *99*, 83–97. [[CrossRef](#)]
11. Milonjić, S.K.; Ruvarac, A.L.; Šušić, M.V. The heat of immersion of natural magnetite in aqueous solutions. *Thermochim. Acta* **1975**, *11*, 261–266. [[CrossRef](#)]
12. Lazarević, S. The Influence of Modification Methods on Physico-Chemical and Sorption Properties of Sepiolite. Ph.D. Thesis, Faculty of Technology and Metallurgy, Belgrade, Serbia, 2012.
13. Jin, H.; Capared, S.; Chang, Z.; Gao, J.; Xu, Y.; Zhang, J. Biochar pyrolytically produced from municipal solid wastes for aqueous As(V) removal: Adsorption property and its improvement with KOH activation. *Bioresour. Technol.* **2014**, *169*, 622–629. [[CrossRef](#)] [[PubMed](#)]
14. Ciannamea, E.M.; Stefani, P.M.; Ruseckaite, R.A. Medium-density particleboards from modified rice husks and soybean protein concentrate-based adhesives. *Bioresour. Technol.* **2010**, *101*, 818–825.
15. Šoštarčić, T.; Petrović, M.; Pastor, F.; Lončarević, D.; Petrović, J.; Milojković, J.; Stojanović, M. Study of heavy metals biosorption on native and alkali-treated apricot shells and its application in wastewater treatment. *J. Mol. Liq.* **2018**, *259*, 340–349. [[CrossRef](#)]
16. Chen, H.; Dai, G.; Zhao, J.; Zhong, A.; Wu, J.; Yan, H. Removal of copper (II) ions by a bio-sorbent—*Cinnamomum camphora*. *J. Hazard. Mater.* **2010**, *177*, 228–236. [[CrossRef](#)]
17. Lagergren, S. Zur theorie der sogenannten adsorption gel ster stoffe. *K. Sven. Vetenskapsakad. Handl.* **1898**, *24*, 1–39.
18. Weber, W.; Morris, J. Kinetics of adsorption on carbon from solution. *J. Sanit. Eng. Div.* **1963**, *89*, 31–60. [[CrossRef](#)]
19. Ho, Y.S.; McKay, G. Pseudo-second order model for sorption processes. *Process Biochem.* **1999**, *34*, 451–465. [[CrossRef](#)]
20. Banat, F.; Sameer, A.A.; Leema, A.M. Utilization of raw and activated date pits for the removal of phenol from aqueous solution. *Chem. Eng. Technol.* **2004**, *27*, 80–86. [[CrossRef](#)]
21. Chairata, M.; Saowanee, R.; Bremner, J.B.; Rattanaphani, V. An adsorption and kinetic study of lac dyeing on silk. *Dyes Pigm.* **2005**, *64*, 231–241. [[CrossRef](#)]
22. Elkady, M.F.; Ibrahim, A.M.; El-Latif, M.M.A. Assessment of the adsorption kinetics, equilibrium and thermodynamic for the potential removal of reactive red dye using eggshell biocompo-site beads. *Desalination* **2011**, *278*, 412–423. [[CrossRef](#)]
23. Cheung, W.H.; Szeto, S.Z.; McKay, G. Intraparticle diffusion processes during acid dye adsorption onto chitosan. *Bioresour. Technol.* **2007**, *98*, 2897–2904. [[CrossRef](#)] [[PubMed](#)]
24. Langmuir, I. The adsorption of gases on plane surfaces of glass, mica and platinum. *J. Am. Chem. Soc.* **1918**, *40*, 1361–1403. [[CrossRef](#)]
25. Webber, T.W.; Chakravorti, R.K. Pore and solid diffusion models for fixed-bed adsorbers. *AIChE J.* **1974**, *20*, 228–238. [[CrossRef](#)]
26. Foo, K.Y.; Hameed, B.H. Insights into the modeling of adsorption isotherm systems. *Chem. Eng. J.* **2010**, *156*, 2–10. [[CrossRef](#)]
27. Freundlich, H.M.F. Über die adsorption in lösungen. *Z. Phys. Chem.* **1906**, *57A*, 385–470. [[CrossRef](#)]
28. Dubinin, M.M.; Radushkevich, L.V. The equation of the characteristic curve of the activated charcoal. *Proc. Acad. Sci. USSR Phys. Chem. Sect.* **1947**, *55*, 331–337.
29. Tempkin, M.J.; Pyzhev, V. Recent modifications to Langmuir isotherms. *Acta Physiochim. URSS* **1940**, *12*, 217–222.
30. Sips, R. On the structure of a catalyst surface. *J. Chem. Phys.* **1948**, *16*, 490–495. [[CrossRef](#)]
31. Redlich, O.; Peterson, D. A useful adsorption isotherm. *J. Phys. Chem.* **1959**, *63*, 1024–1027. [[CrossRef](#)]
32. Gorgievski, M.; Božić, D.; Stanković, V.; Štrbac, N.; Šerbula, S. Kinetics, equilibrium and mechanism of Cu^{2+} , Ni^{2+} and Zn^{2+} ions biosorption using wheat straw. *Ecol. Eng.* **2013**, *58*, 113–122. [[CrossRef](#)]
33. Villaescusa, I.; Fiol, N.; Martínez, M.; Miralles, N.; Poch, J.; Serarols, J. Removal of copper and nickel ions from aqueous solutions by grape stalks wastes. *Water Res.* **2004**, *38*, 992–1002. [[CrossRef](#)] [[PubMed](#)]